Published online 26 February 2013 *Nucleic Acids Research, 2013, Vol. 41, No. 8* ***4729–4739***
doi:10.1093/nar/gkt121

Pseudo-complementary PNA actuators as reversible switches in dynamic DNA nanotechnology

Damian Ackermann and Michael Famulok*

Chemical Biology and Medicinal Chemistry Unit, LIMES Institute, c/o Kekulé Institute of Organic Chemistry and Biochemistry, University of Bonn, Gerhard-Domagk-Strasse 1, 53121 Bonn, Germany

Received November 8, 2012; Revised January 23, 2013; Accepted February 7, 2013

ABSTRACT

The structural reorganization of nanoscale DNA architectures is a fundamental aspect in dynamic DNA nanotechnology. Commonly, DNA nanoarchitectures are reorganized by means of toehold-expanded DNA sequences in a strand exchange process. Here we describe an unprecedented, toehold-free switching process that relies on pseudo-complementary peptide nucleic acid (pcPNA) by using a mechanism that involves double-strand invasion. The usefulness of this approach is demonstrated by application of these peptide nucleic acids (PNAs) as switches in a DNA rotaxane architecture. The monomers required for generating the pcPNA were obtained by an improved synthesis strategy and were incorporated into a PNA actuator sequence as well as into a short DNA strand that subsequently was integrated into the rotaxane architecture. Alternate addition of a DNA and PNA actuator sequence allowed the multiple reversible switching between a mobile rotaxane macrocycle and a stationary pseudorotaxane state. The switching occurs in an isothermal process at room temperature and is nearly quantitative in each switching step. pcPNAs can potentially be combined with light- and toehold-based switches, thus broadening the toolbox of orthogonal switching approaches for DNA architectures that open up new avenues in dynamic DNA nanotechnology.

INTRODUCTION

The development of dynamic nanoscale DNA architectures currently represents a focal point in DNA nanotechnology (1–8) [for reviews see (9–12)]. In this context, 'dynamic' denotes the well-directed reorganization of a defined DNA architecture in which both the geometry and the intrinsic structure-determined functions are altered. In most cases, this structural reorganization is achieved by a strand-exchange approach by means of toehold-expanded DNA sequences (13–18). The toehold itself not only serves as a recognition sequence, but also advances the structural transformation under thermodynamic control by pairing with a fully complementary counter strand. Toehold-driven systems can usually be operated in a reversible fashion, but they underlie certain experimental restrictions, such as the gradual dilution of the sample. Recent developments in toehold-mediated strand displacement like the remote toehold approach (19) or the associative toehold activation (20) direct towards improved control of the displacement kinetics.

In principle, repetitive switching by light-triggered structural interconversions based on azobenzene-modified DNA sequences can circumvent these restrictions. Hitherto existing applications have shown that architecturally simpler DNA nanostructures like molecular tweezers (21) and beacons (22), DNAzymes (23,24) or DNA tetrahedrons (25) are suited for light-induced switching, but this has not yet been implemented for the switching of more complex origami-based DNA structures. By using a double-stranded DNA (dsDNA) rotaxane architecture (26) that we reversibly switched between a mobile and stalled macrocycle, we have recently shown that light-induced switching operations based on dimethylazobenzene (DMAB)-functionalized DNA sequences result in a more robust switching behavior than oligodeoxynucleotides (ODNs) functionalized with unmodified azobenzene (27), and thus may find broader applications in DNA nanotechnology. Despite the advantage of light-triggered switching with DMAB-ODNs, their application is restricted to an individual switching function. In cases in which different switches are to be operated in an independent, orthogonal fashion within a DNA nanoarchitecture, the DMAB-based light-trigger comes to its limits. Even though achievements towards this goal have been reported (28), there are currently no systems that can be operated at different wavelengths completely orthogonally.

Moreover, the demand for novel tools for the reversible switching of DNA nanoarchitectures is also illustrated by

*To whom correspondence should be addressed. Tel: +49 228 731 787; Fax: +49 228 735 388; Email: m.famulok@uni-bonn.de

a recent report that the wedge-face porosity in a DNA tetrahedron could be directed through a toehold-free exchange mechanism (29). To augment the spectrum of reversible switching mechanisms for DNA nanotechnology even further, our aim is to find novel principles of switching devices that can be used orthogonally to the currently available methods. Here we report such a novel principle, based on DNA double-strand invasion that relies on the precisely tuned interaction of pseudo-complementary (pc) nucleobases. The design strategy of this novel switching mechanism was programmed into a DNA rotaxane in which a threaded DNA macrocycle can be switched back and forth between mobile and immobile states, and that serves as our test system for dynamic DNA nanotechnology (Figure 1a).

The concept of pc nucleobases goes back to Gamper and colleagues (30) and has meanwhile found application even in polymerase chain reaction (31). Thereby, on one hand, a thymine (T) is substituted for a 2-thiouridine (S),

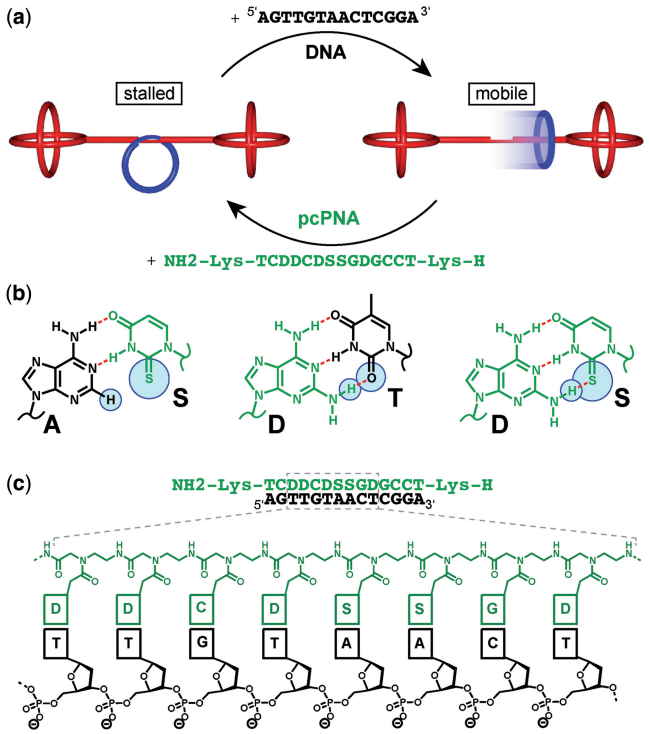

Figure 1. Design of pseudo-complementary PNA actuators for reversible switching of DNA nanoarchitectures. (**a**) pcPNA-controlled reversible nanomechanical switch. Addition of the DNA 'release oligo' (black) detaches the macrocycle (blue) from the dumbbell (red) forming the genuine rotaxane (mobile). Subsequently, added pcPNA (green) invades the macrocycle and the gap ring (blue) binds back to the dumbbell to form the original pseudorotaxane (stalled). (**b**) Base pairing motif of pc nucleobases. 2-Thiouracil (S) and adenine (A) form a stable S•A base pair. 2,6-diaminopurine (D) pairs with thymine (T) by forming three hydrogen bonds. Due to a steric clash between the sulphur atom of S and the additional amino group of D, the corresponding S•D base pair is not stable. Therefore, self-pairing of nucleic acid sequences containing pc nucleobases is strongly suppressed compared with cross-pairing with unmodified ODNs. (**c**) Chemical structure of the anti-parallel arranged PNA•DNA hybrid. In each switching cycle, the thermodynamically most stable pcPNA•DNA hybrid is formed.

whereas on the other hand, an adenine (A) is changed for a 2,6-diaminopurine (D) residue (Figure 1b). Due to an unfavourable steric interaction between the additional amino group in the 2,6-diaminopurine and the sulphur atom in the 2-thiouridine residue, the base pairing between the two pc nucleobases S and D is prevented. The cross-pairing S•A is still possible, whereas the pairing D•T is even stronger than in the unmodified A•T pair, owing to the third hydrogen bond (Figure 1b). This pairing behaviour of pcDNA sequences results in the invasion at the end of a natural DNA double strand and in the branching of the DNA structure (30). Nielsen subsequently incorporated the pc nucleobases into peptide nucleic acids (32,33) [PNA; for reviews see (34–37)] and showed that pseudo-complementary PNA (pcPNA) binds with high sequence specificity to dsDNA through double-duplex invasion (38,39). This observation correlates with the fact that hybrid double strands of PNA•DNA are thermodynamically more stable than the corresponding DNA•DNA double strands (30,38,40).

In our rotaxane model system, however, the pcPNA is not used for addressing dsDNA through the principle of double-duplex invasion. Instead, it is used as an actuator that binds to a 14-mer DNA sequence, termed 'release ODN' (RO). The RO is complementary to the short single-stranded gap in the macrocycle, to which it hybridizes and thereby releases it from its complementary hybridization site at the axle of the dumbbell. Binding of the pcPNA to the RO in turn removes the RO from the macrocycle, which now can hybridize back to the axle, and the architecture reorganizes into the stalled pseudorotaxane state. This switching cycle between a stalled and mobile macrocycle is fuelled by the formation of the thermodynamically more stable pcPNA•DNA hybrid duplex (Figure 1c). In this way it is possible to switch back and forth between the fixed and mobile macrocycle in the rotaxane architecture. This mode of switching is unprecedented in DNA nanotechnology. Because it differs mechanistically both from the toehold as well as from the light-induced azobenzene switch, it can potentially be combined orthogonally with these switching approaches.

MATERIALS AND METHODS

General

Standard DNA sequences used to assemble the rotaxane were ordered as 5′-phosphorylated ODNs in high-performance liquid chromatography (HPLC) quality from Metabion (see Supplementary Table S1 for the sequences). 1× TAE buffer: 40 mM Tris, 20 mM AcOH, 1 mM EDTA. 1× Seeman buffer: 40 mM Tris, 20 mM AcOH, 12.5 mM $MgCl_2$, 2.5 mM EDTA. 1× DNA storage buffer: 10 mM Tris•HCl, 50 mM NaCl, pH 7.5. Gel loading buffer: 0.01% bromophenol blue and 0.01% xylene cyanol in glycerol/H_2O 1:1. Gels were stained with ethidium bromide and visualized by ultraviolet irradiation.

Polyacrylamide gel electrophoresis

Equipment: Mini-Protean III (Bio-Rad). Preparation of 10% gels: a 30% aq. acrylamide/bisacrylamide (37.5:1) soln. (4.0 ml, Carl Roth GmbH) was diluted with 10× TAE (1.2 ml) and H_2O (6.8 ml), treated with a 10% aq ammonium persulfate soln. (50 µl) and *N*,*N*,*N*′,*N*′-tetramethylethylenediamine (10 µl) and then polymerized for 1 h. Sample preparation: 2 µl sample was mixed with 1 µl gel loading buffer. The gel was run at 150 V for 1 h at room temperature (RT).

Agarose gel electrophoresis

Equipment: Owl B1 EasyCast Mini Gel System (Owl Separation Systems). Preparation of 2.4% gels: high-resolution agarose (900 mg, Carl Roth GmbH) was suspended in 0.5× TAE (37.5 ml), melted and then poured in the horizontal chamber. Sample preparation: 5 µl sample was mixed with 1 µl gel loading buffer at 4°C. Gels were run at 150 V for 2 h at 4°C.

HPLC purification of DNA architectures

Weak anion-exchange (WAX)-HPLC: column TSKgel DEAE-NPR (4.6 × 35 mm, Tosoh); buffer WAX-A: 20 mM Tris·HCl, pH 9.0; buffer WAX-B: 20 mM Tris·HCl, 1.0 M NaCl, pH 9.0; gradient 40–65% WAX-B in 30 min. After purification, the fractions were concentrated using Ultracel centrifugal filters (YM-30, YM-100, Millipore), washed 2× with DNA storage buffer and stored in 100 µl DNA storage buffer.

Synthesis of monomers

***Ethyl-N-(2-(t-butyloxycarbonylamino)ethyl)-N-(2-amino-6-chloropurin-9-ylacetyl)glycinate* (6)**

A solution of **5** (1.77 g, 7.8 mmol) and EtN^iPr_2 (1.21 g, 9.4 mmol) in DMF (15 ml) was treated with *O*-(benzotriazol-1-yl)-*N*,*N*,*N*′,*N*′-tetramethyluronium hexafluorophosphate (3.25 g, 8.5 mmol) for 5 min at RT. Then a solution of ethyl *N*-(*t*-butyloxycarbonyl [Boc]-aminoethyl) glycinate (2.11 g, 8.5 mmol) in DMF (5 ml) was added and the mixture stirred at RT for 3 h. The mixture was partitioned between CH_2Cl_2 and sat. aq. $NaHCO_3$ soln., the organic layer washed with 10% aq. citric acid soln., dried with $MgSO_4$ and evaporated under reduced pressure. The crude was adsorbed on SiO_2 (14 g). Column chromatography (CC) [silica gel (30 g), hexane/AcOEt 1:1 → AcOEt → AcOEt/MeOH 98:2] gave **6** (3.45 g, 97%) as yellow foam. ^{1}H-NMR (400 MHz, DMSO-d6) δ 7.96 and 7.95 [s, major and minor rotamer (maj/min), respectively, 1H, H-C(8)], 7.00 and 6.74 [t, J = 7.0 Hz, (maj/min), 1H, NH], 6.88 and 6.64 [br. s, (maj/min), 2H, NH_2], 5.14 and 5.11 and 4.79 and 4.59 [s (four rotamers) 2H, $CH_2N(9)$], 4.41 and 4.06 [s (maj/min), 2H, CH_2COOEt], 4.20 and 4.07 [q, J = 7.1 Hz, (min/maj), 2H, OCH_2CH_3], 3.50 and 3.34 and 3.25 and 3.01 [2m, (maj/min), minor peak overlaps with HDO signal, 4H, NCH_2CH_2N], 1.37 and 1.35 [s (maj/min), 9H, $C(CH_3)_3$], 1.25 and 1.16 [q, J = 7.1 Hz, (min/maj), 3H, OCH_2CH_3]. ^{13}C-NMR (101 MHz, DMSO-d6) δ 169.43 and 168.93 (min/maj), 167.09 and 166.74 (min/maj), 159.82 and 159.80 (min/maj), 155.79 and 155.58 (maj/min), 154.53, 149.29 and 149.26 (min/maj), 143.96 and 143.86 (min/maj), 128.33 and 128.31 (maj/min), 78.17 and 77.82 (maj/min), 61.30 and 60.61 (min/maj), 49.17 and 47.95 (min/maj), 47.02 and 46.95 (maj/min), 43.92 and 43.56 (min/maj), 38.38 and 37.68 (maj/min), 28.22 and 28.19 (min/maj), 14.06 and 14.04 (min/maj). Electrospray ionization mass spectrometry (ESI-MS) (pos.) 456.3 ($[M+H]^+$, $C_{18}H_{27}ClN_7O_5^+$; calc. 456.2).

***Ethyl-N-(2-(t-butyloxycarbonylamino)ethyl)-N-(2,6-diaminopurin-9-ylacetyl)glycinate* (7)**

A solution of **6** (4.60 g, 10.0 mmol) in DMSO was treated with NaN_3 (1.31 g, 20 mmol) at 90°C for 2 h. The mixture was cooled to 65°C and reacted with PPh_3 (6.61 g, 25 mmol) for 3 h. The solution was diluted with CH_2Cl_2 (100 ml), washed with sat. aq. $NaHCO_3$ soln., dried with $MgSO_4$ and evaporated to dryness. The crude was dissolved in MeOH/THF/1.0 M aq. triethylammonium acetate (TEAA) soln. (5:5:2, 60 ml) and stirred at 65°C overnight, concentrated to 15 ml. The remaining mixture was separated between CH_2Cl_2 (200 ml) and sat. aq. NaCl soln. (200 ml), the organic layer dried with $MgSO_4$, and the solvent evaporated under reduced pressure. The crude was adsorbed on SiO_2 (7 g). CC [silica gel (35 g), CH_2Cl_2→MeOH/CH_2Cl_2 88:12] gave **7** (2.79 g, 63%) as white powder. ^{1}H-NMR (300 MHz, DMSO-d6) δ 7.54 and 7.53 [s, major and minor rotamer (maj/min), respectively, 1H, H-C(8)], 7.00 and 6.75 [t, J = 7.0 Hz, (maj/min), 1H, NH], 6.65 (s, 2H, NH_2), 5.73 (s, 2H, NH_2), 4.97 and 4.80 [s (maj/min), 2H, $CH_2N(9)$], 4.39 and 4.05 [s (maj/min), 2H, CH_2COOEt], 4.18 and 4.06 [q, J = 7.1 Hz, (min/maj), 2H, OCH_2CH_3], 3.50 and 3.30 [m, (maj/min), minor peak overlaps with HDO signal, 2H, NCH_2], 3.23 and 3.03 [m, (maj/min), 2H, NCH_2], 1.37 and 1.36 [s (maj/min), 9H, $C(CH_3)_3$], 1.25 and 1.19 [q, J = 7.1 Hz, (min/maj), 3H, OCH_2CH_3]. ^{13}C-NMR (75 MHz, DMSO-d6) δ 169.90 and 169.47 (min/maj), 168.02 and 167.68 (min/maj), 160.63 and 160.61 (maj/min), 156.45, 156.18 and 155.99 (maj/min), 152.54 and 152.52 (maj/min), 138.57 and 138.52 (min/maj), 113.02 and 113.00 (maj/min), 78.53 and 78.19 (maj/min), 61.64 and 60.96 (min/maj), 55.32, 49.63, 48.22, 47.42, 43.63 and 43.21 (min/maj), 28.63 and 28.59 (maj/min), 14.44. ESI-MS (pos.) 437.3 ($[M+H]^+$, $C_{18}H_{29}N_8O_5^+$; calc. 437.2).

***N-(2-(t-Butyloxycarbonylamino)ethyl)-N-(2-amino-6-(benzyloxycarbonylamino)purin-9-ylacetyl)glycine* (2)**

7 (2.79 g, 6.4 mmol) was dissolved in CH_2Cl_2/dioxane (1:2) at elevated temperature, cooled to RT and treated with EtN^iPr_2 (0.91 g, 7.0 mmol) and *N*-benzyloxycarbonyl (Z)-*N*′-methylimidazolium triflate (4.68 g, 6.8 mmol, Rapoport reagent) overnight. The reaction was quenched by addition of MeOH (5 ml), and the solvents were removed by evaporation. The crude was adsorbed on SiO_2 (6 g). CC [silica gel (40 g), CH_2Cl_2→MeOH/CH_2Cl_2 94:6] gave ethyl-*N*-(2-(Boc-amino)ethyl)-*N*-(2-amino-6-(benzyloxycarbonylamino)purin-9-ylacetyl)glycinate (3.30 g, 90%). This intermediate (3.2 g, 5.6 mmol) was dissolved in THF/H_2O 2:1 (75 ml), treated with 2.0 M aq. NaOH soln. (4.2 ml) and stirred for 30 min. THF

was removed under reduced pressure, the aq. layer cooled to 0°C and adjusted to pH 4 using 1.0 M HCl. The precipitate was filtered, washed with water and dried in vacuo to give **2** (2.12 g, 70%) as white solid. ^{1}H-NMR (400 MHz, DMSO-d6) δ 12.74 (br. s, 1H, COOH), 10.16 (br. s, 1H, arom. C(1)NH), 7.81 (s, 1H, H-C(8)), 7.45 - 7.36 (m, 5H, arom. H), 7.01 and 6.76 (t, J = 7.0, NH), 6.38 (br. s, 2H, C(3)NH_2), 5.17 (s, 2H, CH_2Bn), 5.06 and 4.89 [s (maj/min), 2H, CH_2N(9)], 4.30 and 3.99 [s (min/maj), 2H, CH_2COOEt], 3.49 and 3.31 [m (maj/min), minor peak overlaps with HDO signal, 2H, NCH_2], 3.26 and 3.04 [s (min/maj), 2H, NCH_2], 1.36 and 1.35 [s (maj/min), 9H, C(CH_3)$_3$]. ^{13}C-NMR (101 MHz, DMSO-d6) δ 170.91 and 170.48 (min/maj), 167.25 and 166.81 (min/maj), 159.72, 155.80 and 155.61 (maj/min), 154.45, 152.43, 149.78 and 149.74 (maj/min), 141.33 and 141.21 (min/maj), 136.59, 128.34, 127.90, 127.82, 116.74 and 116.71 (maj/min), 78.14 and 77.81 (maj/min), 66.00, 49.20, 47.68, 47.00 and 46.89 (min/maj), 43.43 and 43.14 (maj/min), 38.29 and 37.61 (maj/min), 28.24 and 28.21 (maj/min). ESI-MS (pos.) 543.4 ([M+H]$^+$, $C_{24}H_{31}N_8O_7^+$; calc. 543.2).

***S-(4-(Acetoxybenzyl)-2-thiothymine* (9)**

2-Thiothymine (3.5 g, 24.6 mmol), 4-(chloromethyl)phenyl acetate (5.0 g, 27 mmol) and potassium carbonate (5.1 g, 36.8 mmol) were suspended in acetone (50 ml) and refluxed for 3 h. The acetone was removed, the crude partitioned between CH_2Cl_2 and 10% aq. citric acid soln., the organic layer dried with $MgSO_4$ and evaporated under reduced pressure. Recrystallization from CH_2Cl_2/CCl_4 (1:2, 80 ml) gave **9** as white crystals (4.03 g, 57%). ^{1}H-NMR (300 MHz, DMSO-d6) δ 12.66 (s, 1H, NH), 12.66 (s, 1H, NH), 7.77 (s, 1H, H-C(6)), 7.42 (m, 2H, arom. H), 7.05 (m, 2H, arom. H), 4.37 (s, 2H, CH_2), 2.24 (s, 3H, OCH_3), 1.86 (s, 3H, C(5)-CH_3). ^{13}C-NMR (75 MHz, DMSO-d6) δ 169.16, 149.61, 134.89, 130.03, 121.81, 32.82, 20.83, 12.50. ESI-MS (pos.) 291.1 ([M+H]$^+$, $C_{14}H_{15}N_2O_3S^+$; calc. 291.1).

***2-Thiothymidine* (10)**

9 (3.2 g, 11.0 mM) and bis(trimethylsilyl) acetamide (2.97 g, 14.6 mmol) were suspended in CH_2Cl_2 (50 ml) and stirred until the solution turned clear. 1-Chloro-2-deoxy-3,5-di-*O*-toluoyl-α-D-ribofuranose (2.84 g, 7.3 mmol) was added, and after cooling to 4°C, the mixture was treated with $SnCl_4$ (1.28 ml, 11.0 mmol) for 1 h at 4°C. After quenching the reaction by the addition of sat. aq. $NaHCO_3$ soln. (100 ml), the organic layer was diluted with CH_2Cl_2 (100 ml), separated and dried with $MgSO_4$ and evaporated under reduced pressure. The crude was dissolved in MeOH/THF 1:1 (200 ml). After addition of 1.0 M aq. NaOH soln. (40 ml), the mixture was stirred for 30 min at RT and then neutralized by adding aq. citric acid soln. (4.0 g in 20 ml H_2O). All solvents were removed under reduced pressure. The remaining solid was dissolved in MeOH, dried with $MgSO_4$ and adsorbed on SiO_2 (10 g). CC (silica gel (50 g), hexane/AcOEt 1:1 → AcOEt) gave a mixture of **10** and the α-*S*-nucleoside (1.35 g). The mixture was further purified by recrystallization from EtOH/$(CH_2Cl)_2$ (1:1, 80 ml) to give **10** (750 mg, 40%) as fine crystals. ^{1}H-NMR (400 MHz, DMSO-d6) δ 12.55 (s, 1H, NH), 8.00 (s, 1H, H-C(6)), 6.83 (t, J = 6.4 Hz, 1H, H-C(1′)), 5.26 (d, J = 4.2 Hz, 1H, C(3′)OH), 5.17 (t, J = 5.0 Hz, 1H, C(5′)OH), 4.25 (m, 1H, H-C(3′)), 3.86 (m, 1H, H-C(4′)), 3.63 (qdd, J = 12.0, 4.9, 3.4 Hz, 2H, H-C(2′)), 2.24 (ddd, J = 13.3, 6.1, 3.6 Hz, 1H, H-C(5′)), 2.02 (ddd, J = 13.3, 7.1, 6.2 Hz, 1H, H′-C(5′)), 1.81 (s, 3H, CH_3). ^{13}C-NMR (75 MHz, DMSO-d6) δ 174.21, 160.63, 136.72, 115.19, 89.14, 87.95, 69.84, 60.77, 40.05 (overlaps with DMSO signal), 12.60. ESI-MS (pos.) 259.0 ([M+H]$^+$, $C_{10}H_{15}N_2O_4S^+$; calc. 259.1).

***1-[2′-Deoxy-5′-O-(4,4′-dimethoxytrityl)-β-D-ribofuranosyl]-2-thiothymine 3′-(2-cyanoethyl diisopropylphosphoramidite)* (3)**

A solution of 2-thiothymidine (647 mg, 2.5 mmol), 4-(dimethylamino)pyridine (61 mg, 0.5 mmol) and 4,4′-dimethoxytrityl chloride (1020 mg, 3.0 mmol) in pyridine (10 ml) was stirred 18 h at RT. After quenching with MeOH (500 µl), the pyridine was removed by co-evaporation with toluene (3×). The residual oil was dissolved in CH_2Cl_2 and then adsorbed on SiO_2 (2 g). CC [silica gel (15 g), hexane/AcOEt 1:1 (+2% Et_3N) → AcOEt (+2% Et_3N)] gave 1-[2′-deoxy-5′-*O*-(4,4′-dimethoxytrityl)-β-D-ribofuranosyl]-2-thiothymine (1.21 g, 86%). The intermediate (1.12 g, 2.0 mmol) was dissolved in CH_2Cl_2 (20 ml) and treated with Et$N^i$$Pr_2$ (860 µl, 5.0 mmol) and 2-cyanoethyl di-isopropylphosphoramidochloridite (570 mg, 2.4 mmol). After stirring for 18 h at RT, the solution was directly subjected to CC [silica gel (20 g), hexane/AcOEt 7:3 (+ 2% Et_3N) → hexane/AcOEt 1:9 (+ 2% Et_3N)], which gave **3** (1.27 g, 84%) as white foam. ^{1}H-NMR (400 MHz, $CDCl_3$) δ 9.34 (br. s, 1H), 7.85 and 7.81 (2s, 1H, NH), 7.34 - 7.31 (m, 2H, H-C(6)), 7.26 - 7.18 (m, 7H), 6.89 - 6.83 (m, 1H, H-C(1′)), 6.79 - 6.74 (m, 4H), 4.64 - 4.56 (m, 1H, H-C(3′)), 4.14 - 4.10 (m, 1H, H-C(4′)), 3.79 - 3.67 (m, 1H), 3.73 and 3.72 (2s, 6H), 3.58 - 3.47 (m, 3H), 3.31 - 3.25 (m, 1H), 2.71 - 2.58 (m, 1H), 2.56 (t, J = 6.2 Hz, 1H), 2.35 (t, J = 6.4 Hz, 1H), 2.25 - 2.20 (m, 1H), 1.36 and 1.34 (2s, 3H, C(5)CH_3), 1.10 and 1.09 and 0.98 (3d, J = 6.8 Hz, 12H). ^{13}C-NMR (101 MHz, $CDCl_3$) δ 174.11, 174.03, 160.52, 160.49, 158.75, 158.73, 158.72, 144.12, 136.43, 135.20, 135.19, 135.17, 130.15, 130.14, 130.07, 128.21, 128.12, 127.97, 127.93, 127.21, 117.51, 117.33, 116.55, 116.50, 113.26, 113.24, 113.22, 89.82, 86.96, 86.94, 85.99, 85.94, 85.79, 85.73, 73.01, 72.84, 72.63, 72.46, 62.63, 62.35, 58.39, 58.23, 58.21, 58.04, 55.26, 55.23, 43.37, 43.27, 43.24, 43.15, 40.17, 40.14, 40.04, 40.00, 24.62, 24.58, 24.55, 24.50, 24.47, 24.46, 20.46, 20.39, 20.21, 20.14, 11.95, 11.93. ^{31}P-NMR (162 MHz, $CDCl_3$) δ 149.99, 149.20. ESI-MS (pos.) 761.5 ([M+H]$^+$, $C_{40}H_{50}N_4O_7PS^+$; calc. 761.3).

Synthesis of psiPNA by solid-phase peptide synthesis

psiPNA was assembled on a PS3 peptide synthesizer (Peptide Instruments) using Boc-solid-phase peptide synthesis analogous protocols (37). PNA monomers (ASM research chemicals): Boc-C(Z)-OH, Boc-G(Z)-OH, Boc-T-OH; lysine monomer: Boc-Lys(2ClZ)-OH (Novabiochem). Synthesis scale: 10 µmol; resin: 4-methylbenzhydrylamine

(resin) (10 mg, 1.1 mmol NH_2/g, pre-swelling in DMF for 1 h); monomer soln.: monomer (75 μmol) and diethyl cyclohexylamine (200 μmol) in 1.0 ml pyridine; activator soln. (per coupling): *O*-(benzotriazol-1-yl)-*N*,*N*,*N*′,*N*′-tetramethyluronium hexafluorophosphate (69 μmol) in DMF (3.0 ml); Boc deprotection soln.: trifluoroacetic acid (TFA)/CH_2Cl_2 1:1. Coupling cycle: mix monomer soln. with activator soln. for 1 min. before loading on resin; couple for 30 min; washing step (first DMF then CH_2Cl_2); Boc deprotection (2 × 12 min, 2 × 5 ml); washing step (first CH_2Cl_2 then DMF). Cycles were run without capping step. Final deprotection and cleavage from resin: soln. A: TFA/dimethyl sulfide/*m*-cresol (2:6:2, v/v/v); soln. B: TFA/trifluoromethanesulfonic acid (9:1, v/v); wash resin with TFA (200 μl); treat resin with a mixture A/B 1:1 (800 μl) for 1 h at RT; filter resin; rinse with TFA (100 μl); add soln. B (600 μl) to resin and shake for 1.0 h at RT; separate resin from solution by filtration through glass wool and transfer the liquid in fresh vial; precipitate PNA by adding Et_2O (3.0 ml); centrifuge and wash pellet 2× with Et_2O; dissolve pellet in 0.1% aq. TFA soln. (1.0 ml). psiPNA was purified by HPLC; column RP-C18 (Zorbax SB-Aq, 4.6 × 150 mm); buffer A: 0.1% TFA in H_2O; buffer B: CH_3CN; gradient: 0–30% B in 20 min. The purified psiPNA was stored in 0.1% aq. TFA soln. (500 μl, buffer A). ESI-MS (m/z, pos.) 4091.8 ($[M+H]^+$, calc. 4091.2).

Synthesis of pcDNA sequences SD5-DNA and pc-anti-RO

The DNA oligomers were synthesized on an Applied BioSystems 3400 DNA synthesizer using the phosphoramidite monomers Bz-dA-CE-phosphoramidite, Ac-dC-CE-phosphoramidite, dmf-dG-CE-phosphoramidite, dT-CE-phosphoramidite (all from SACF Proligo Reagents), D: 2-amino-dA-CE phosphoramidite (4, Link Technologies) S: 2-thio-dT-CE-phosphoramidite (3), 5′-phosphitylating reagent (Link Technologies) and dG-CPG support at 0.2 μmol scale. The sequences were prepared according to standard synthetic procedures ('trityl-off' mode), using *t*-BuOOH (1.0 M) in nonane/$(CH_2Cl)_2$ (1:4) as oxidant. 2-Thiothymidine phosphoramidite **3** was used as a 0.1 M soln. in CH_3CN. Coupling time: 30 s. Oxidation time: 60 s. Detritylation time: 60 s. After completion of the synthesis, the product was treated with 10 M $MeNH_2$ in H_2O/EtOH (1:1, 1 ml) for 24 h at RT. After evaporating the solvent, the raw product was dissolved in 100 mM aq. TEAA buffer and purified by reverse phase high-performance liquid chromatography (RP-HPLC); buffer A: 100 mM TEAA in H_2O; buffer B: CH_3CN; gradient: 5–17% B in 20 min. The purified DNA sequences were concentrated to dryness and then re-dissolved in 500 μl H_2O. LC-MS (m/z, neg.): SD5-DNA 6258.3 ($[M-H]^-$, calc. 6254.9); pc-anti-RO 4314.3 ($[M-H]^-$, calc. 4314.0).

Assembly of pcRod

EFCT-1, EFCT-2, rodA-DNA, rodC-DNA and SD5-DNA (1000 pmol each) in 1× ligation buffer (200 μl) were incubated with ligase (40 U, Rapid DNA Ligation Kit, Roche) at RT for 24 h. The assembly was monitored by 10% polyacrylamide gel electrophoresis (PAGE) (Supplementary Figure S1). The raw product was purified by WAX-HPLC, concentrated in Ultracel centrifugal filters (YM-10, Millipore) and stored in 1× Seeman buffer.

Assembly of the rotaxane

The assembly of PGR gap-ring and spherical stoppers were performed as described previously (41) (for secondary structure see Supplementary Figures S2 and S3). pcRod (15.8 pmol) and PGR (31.6 pmol) were incubated in 1× ligase buffer (50 μl) at 15°C overnight. Pre-cooled spherical stoppers (39.5 pmol) in 1× ligase buffer (50 μl) were added, and the sample incubated with T4 DNA ligase (10 U, Fermentas) for 6 h at 15°C (final volume 100 μl). The assembly was monitored by agarose gel (see previously). The pseudorotaxane was purified by WAX-HPLC.

Invasion of psiPNA and pc-anti-RO to the PGR macrocycle

The gap-ring PGR (25 pmol) and PGR-RO (25.0 pmol) were incubated in 10 mM Tris•HCl (pH 8.0) and 30 mM NaCl (100 μl) at 20°C for 30 min. The sample was split in seven aliquots containing 3.5 pmol macrocycle each (14.0 μl). One aliquot was kept as reference; three were treated with 1.0, 2.0 and 4.0 equivalents of psiPNA, and three with 1.0, 2.0 and 4.0 equivalents of pc-anti-RO, respectively. All samples were diluted with 10 mM Tris•HCl (pH 8.0) to 28 μl and then incubated at 20°C. For analysis, 4.0 μl aliquots of the samples were separated on 10% PAGE (see previously) after different incubation conditions: 2 h at 20°C; 4 h at 20°C; 24 h at 20°C; 2 h at 40°C; then 2 min at 60°C.

Switching macrocycle mobility in the rotaxane

All steps were performed at RT in 1× DNA storage buffer. The WAX-purified pseudorotaxane (2.0 pmol) in buffer (30 μl) was treated with PGR-RO (1.0 μl, 4.0 pmol) for 30 min; 10.3 μl of the sample was removed and stored at 4°C (lane 3 and Figure 6c). The remaining soln. (20.6 μl) was incubated with psiPNA (1.35 μl, 10.5 pmol) overnight; 11.0 μl of the sample was removed and stored at 4°C (lane 4). To the remaining solution, PGR-RO (1.6 μl, 6.4 pmol) was added and incubated for another 30 min (lane 5). For analysis of the switching behaviour, the DNA architectures [0.3 pmol of the three samples, the pseudorotaxane (lane 2) and the dumbbell (lane 1)] were separated on 2.4% agarose gel plate at 4°C (see previously).

Atomic force microscopy

Nanowizard 3, JPK Instruments; measuring mode: HyperDrive in liquid; tip: PPP-NCHAuD (Nanosensors); substrate: mica with polyornithine as adhesive.

RESULTS AND DISCUSSION

Design of the switch system

The underlying principle of the pcPNA switching system consists of the pc nucleobases S and D. Figure 2a depicts the secondary structures that are relevant for the

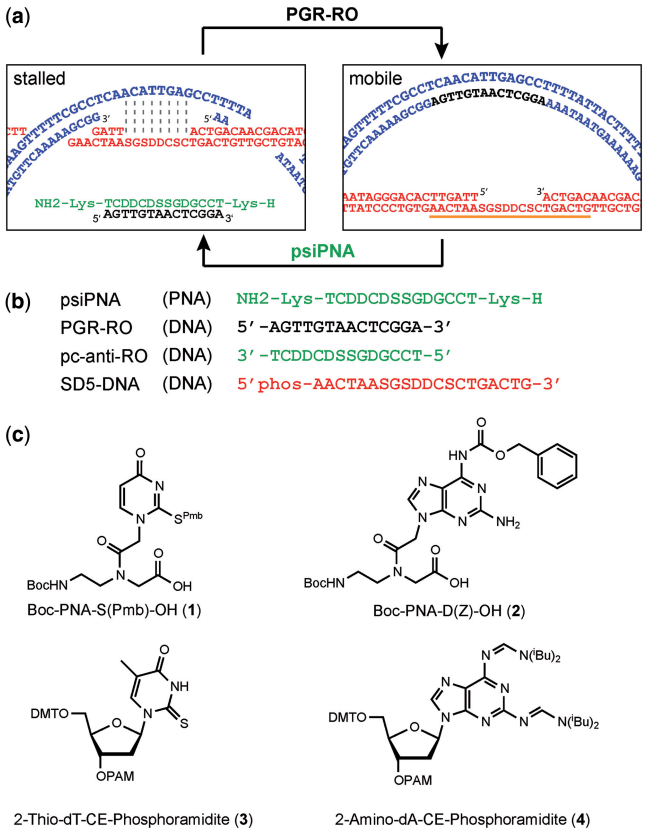

Figure 2. (**a**) Design, mechanism and secondary structure of a nanomechanical switch. In the stalled state, the macrocycle (blue) hybridizes to the axle (red) containing pc nucleobases in the single-stranded region. Addition of PGR-RO (black) displaces the axle from the macrocycle, inducing the mobile state. When psiPNA (green) is added, PGR-RO is detached from the macrocycle in an isothermal invasion process. The gap ring flips back to the axle and the psiPNA•PGR-RO hybrid duplex forms as waste. psiPNA (green) does not bind to the axle (red) because both strands contain pc nucleobases. (**b**) PNA and DNA sequences involved in the switching process. S: 2-Thiouracil for PNA; 2-thiothymine for DNA. D: 2,6-Diaminopurine. (**c**) Chemical structures of PNA and DNA monomers required for the synthesis of pc sequences.

switching of the DNA rotaxane architecture. The left panel illustrates the pseudorotaxane state. The macrocycle (blue) is retained on the axle (red) by base pairing. Note that we are using the term pseudorotaxane because the stationary macrocycle interacts with the axle by base pairing, whereas in the mobile state, these attractive forces between axle and macrocycle are abolished. This nomenclature is in accordance with IUPAC recommendation (42).

The right panel shows the genuine rotaxane state with a mobile macrocycle that is detached because the 14-mer DNA sequence PGR-RO (black) binds to the single-stranded gap in the macrocycle. The importance of the pc nucleobases becomes evident in the second switching event in which the macrocycle is to be fixed again to the axle. To achieve this, the 14-mer PGR-RO needs to be removed from the macrocycle. A natural complementary DNA sequence would preferentially bind to its complementary single-stranded gap region in the axle rather than detaching the PGR-RO from the DNA macrocycle. Therefore, the unmodified DNA system is inherent to collapse. This can be avoided by the use of pc nucleobases for the PNA sequence as well as for the single-stranded gap region in the axle because these two components are unable to hybridize. In contrast, the pairing of the pcPNA with the unmodified 14-mer DNA sequence is still possible. Due to the strongly invasive character of the PNA into dsDNA (43–45), the macrocycle is released from the PGR-RO. As a consequence, the macrocycle hybridizes back to the complementary gap region in the axle to restore the pseudorotaxane.

Synthesis of the pcPNA and DNA sequences

Our switching system relies on base-modified DNA and PNA oligomers (Figure 2b) (32,33,46). The 14-mer PNA actuator sequence 'psiPNA' is accessible through a Boc-protecting group strategy of the pcPNA monomers 2-thiouracil (**1**) and 2,6-diaminopurine (**2**) (Figure 2c; note that 'psiPNA' is the name of the particular PNA sequence used in this study, whereas 'pcPNA' is used as a general term). The three remaining pcPNA monomers Boc-PNA-C(Z)-OH, Boc-PNA-G(Z)-OH and Boc-PNA-T-OH are commercially available. The 2-thiouracil monomer (**1**) was synthesized using a protocol (33,46) that was modified in the first two steps to increase the yield during the introduction of the sulphur-protecting group and the alkylation of the nucleobase with ethyl bromoacetate (Supplementary Methods).

The 2,6-diaminopurine monomer was obtained in a new, short and efficient reaction sequence that clearly differs from previous ones (32,33,46) through the use of 2-amino-6-chloro-9H-purine-9-acetic acid (**5**) as starting material. **5** was directly coupled to ethyl *N*-(Boc-aminoethyl)-glycinate to yield the intermediate **6**, which then was reacted to the unprotected diaminopurine derivative **7** by a known base transformation (Figure 3). (47) The desired monomer **2** was obtained by CBz protection of the *N*-6-amino group with subsequent ester hydrolysis. The introduction of a lysine residue at the ends of a PNA has been shown to not only increase solubility but also to facilitate the PNA's interaction with DNA (48–52). This was accounted for in the design of our pcPNA sequences by adding a lysine both at the amino- and the carboxy- termini. The assembly of the 14-mer PNA sequence 'psiPNA' was then performed under standard automated PNA-synthesis conditions on a peptide synthesizer (32,34,37,53). The product was purified by RP-HPLC, characterized by ESI-MS and stored as a 1.0 mM stock solution.

The incorporation of the pc nucleobases into the DNA sequences is carried out under standard DNA solid-phase synthesis by using the respective phosphoramidites **3** and **4** (Figure 2c), of which the 2-amino-dA-CE-phosphoramidite (**4**) is commercially available. For the 2-thio-dT-CE-phosphoramidite (**3**), some syntheses are described (54,55), the yields of which, however, are unsatisfying, as several structural isomers are formed during the nucleosidation reaction (56,57). To circumvent these problems, we developed a novel strategy by protecting the 2-thiothymine (**8**) as a thioether (**9**) with a

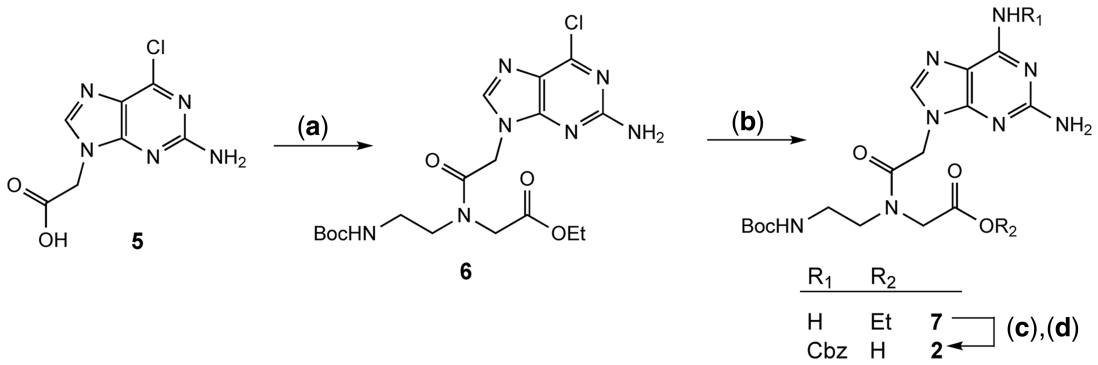

Figure 3. Synthesis of the 2,6-diaminopurine PNA monomer **2.** Reagents: (**a**) Ethyl *N*-(Boc-aminoethyl)glycinate, HBTU, DMF, EtN^iPr_2, RT, 16 h, quantitative. (**b**) (i) NaN_3, DMSO, 90°C, 2 h; (ii) PPh_3, DMSO, 70°C, 3 h; (iii) THF/MeOH/1.0 M TEAA (5:5:2), 60°C, 16 h, 64%. (**c**) Rapoport Reagent, EtN^iPr_2, CH_2Cl_2/dioxane (1:2), RT, 16 h, 90%. (**d**) NaOH, THF/H_2O (2:1), RT, 60 min, 70%.

para-acetoxybenzyl group (Figure 4). This protecting group is usually used for protecting base-sensitive thiols (58,59), but until now, it has not been used for protecting nucleobases. The advantages of the *para*-acetoxybenzyl protecting group for this purpose become evident at several reaction steps: i) it is easy to introduce; ii) both the *S*-2- and the *N*-3 nucleosidation (56) are strongly suppressed; iii) the group is compatible with *Vorbrüggen*-conditions ($SnCl_4$) that preferentially lead to nucleosides in β-configuration at 0°C (54,56,60); iv) its removal can occur without additional reaction steps during ester hydrolysis after nucleosidation. Indeed, the phosphoramidite can be used in the automated DNA synthesis without protecting the sulphur atom if *t*-BuOOH is being used as the oxidation reagent during the coupling cycle (61). A crystal structure of the so obtained nucleoside unambiguously proves the desired configuration (Supplementary Figure S4). The conversion of the 2-thiothymine nucleoside **10** into the phosphoramidite **3** was done by using the standard protocols of nucleotide chemistry (62). The pcDNA sequences SD5-DNA and pc-anti-RO were assembled under standard DNA coupling conditions (31), with the exception that the oxidation step was done with *t*-BuOOH instead of I_2. To prevent desulfuration (63) during the final deprotection step, the DNA sequence was treated with 10 M $MeNH_2$ in H_2O/EtOH (1:1) for 24 h at ambient temperature. The product was purified by RP-HPLC, characterized by ESI-MS and stored as a 100 μM stock solution.

Assembly of the DNA rotaxane

The assembly of the DNA rotaxane occurred by threading of a DNA axle (pcRod) into a dsDNA macrocycle, followed by the ligation of spherical DNA-stoppers at both ends of the pcRod (Figure 5a) (26). The threading is achieved by the formation of eight base pairs between the DNA axle and the gap-containing DNA macrocycle (64), and is a consequence of the helical structure of the dsDNA.

The rotaxane consists of the three components gap ring (PGR; blue), DNA axle (pcRod; black/red) and spherical stoppers (red) (Figure 5a). The spherical stoppers used here were assembled by a recently described one-pot method (41). The criteria for the assembly of the PGR DNA-macrocycle are similar as before (41), but differ in the sequence within the gap region (Supplementary Figure S2). Because the control of the nanomechanical switch occurs at this gap sequence, the corresponding single-stranded region in the pcRod was equipped with pc nucleobases. In this way, these two single-stranded regions fulfil two important functions: (i) they bring about the threading during the assembly of the rotaxane; (ii) they serve the immobilization of the macrocycle when operating the nanomechanical system. The secondary structure of the pcRod sequence is shown in Figure 5b, and consists of five different ODNs. By using EFCT1 and EFCT2 as templates, the three other ODNs rodA-DNA, SD5-DNA and rodC-DNA were ligated to yield pcRod as a continuous DNA strand. A gel-shift analysis (Figure 5c) confirmed that the threading using pc nucleobases occurs as efficiently as when using natural DNA bases. The resulting pseudorotaxane was separated from unreacted starting material by weak ion-exchange HPLC, and the rotaxane architecture was confirmed by high-resolution atomic force microscopy (Figure 5d).

Reversible nanomechanical switching

The implementation of the reversible switching system that consists of the detachment of the PGR-RO from the entirely double-stranded macrocycle constitutes a major challenge. For thermodynamic reasons, the breakup of this continuously double-stranded macrocycle is strongly hindered. The RO can either bind to the complementary DNA gap region to form a DNA•DNA double strand, or to the complementary pcPNA to form a DNA•pcPNA heteroduplex. Therefore, we hypothesize that the detachment of the RO from the macrocycle is thermodynamically favoured if the DNA•pcPNA heteroduplex can form because this heteroduplex is more stable than the DNA•DNA homoduplex. Once the macrocycle is available again with a single-stranded gap region, it can bind back to the complementary sequence on the pcRod to re-establish the initial pseudorotaxane state with an immobile macrocycle. In a pilot study, we compared the displacement efficiencies of the PGR-RO from its hybridization to the PGR macrocycle between psiPNA and the DNA analogue pc-anti-RO (Figure 6a).

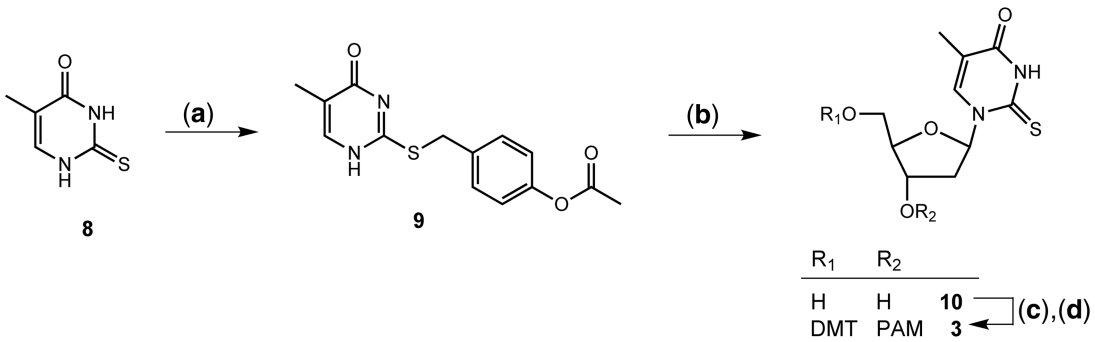

Figure 4. Synthesis of the 2-thio-dT-CE-phosphoramidite **3**. Reagents: (**a**) 4-(Chloromethyl)phenyl acetate, K_2CO_3, acetone, reflux, 3 h, 57%. (**b**) (i) BSA, 1-chloro-2-deoxy-3,5-di-*O*-toluoyl-α-D-ribofuranose, $SnCl_4$, $(CH_2Cl)_2$, 0°C, 1 h; (ii) 0.2 M NaOH, MeOH/THF/H_2O (3:2:1), RT, 30 min, 40%. (**c**) Dimethoxytrityl chloride, DMAP, pyridine, RT, 16 h, 86%. (**d**) 2-Cyanoethyl *N,N*-diisopropylchlorophosphoramidite, EtN^iPr_2, CH_2Cl_2, RT, 16 h, 84%.

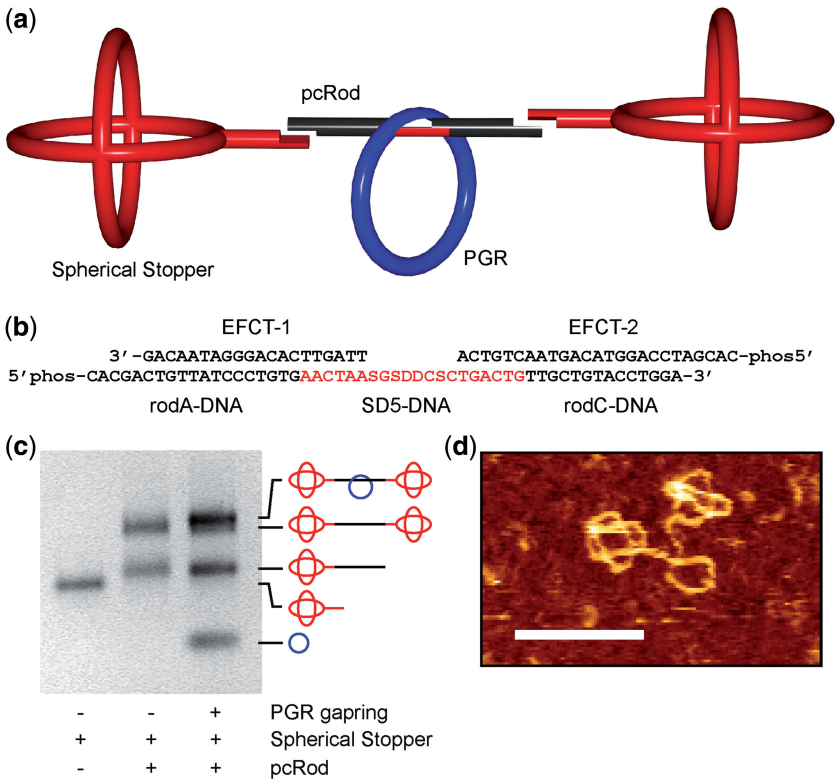

Figure 5. Design of the DNA rotaxane. (**a**) Assembly of the DNA rotaxane from its three components: PGR macrocycle (blue), pcRod (black) and spherical stopper (red). (**b**) Illustration of the secondary structure of pcRod composed of five short ODNs. The pc SD5-DNA (red) is inserted by template-directed ligation. S: Thiothymine; D: Diaminopurine. (**c**) Agarose-gel (2.4%) of the pseudorotaxane assembly. Lane 1: spherical stopper; lane 2: raw product of the dumbbell synthesis; lane 3: raw product of the pseudorotaxane synthesis. The corresponding dumbbell is formed in small amounts only, confirming a high threading efficiency. (**d**) High-resolution AFM picture of the purified pseudorotaxane (scale bar: 50 nm).

For that, the gap macrocycle was provided in solution, incubated for 30 minutes with 1.0 equivalents of PGR-RO and then treated with 1.0, 2.0 and 4.0 equivalents of psiPNA and pc-anti-RO, respectively. Aliquots of these samples were PAGE-separated after different incubation times and temperatures (Figure 6b). We found that in the presence of 4.0 equivalents of psiPNA, the RO is detached from the macrocycle after <2 h at 20°C and the free PGR macrocycle is nearly quantitatively re-established (Figure 6b, upper gel, lane 5). In contrast, the presence of pc-anti-RO had no influence on the macrocycle (lane 6, 7, 8), not even after 24 h (Supplementary Figure S5). When the same samples were warmed up to 60°C for 2 min, the displacement of the RO from the gap ring became more efficient for psiPNA, and started to take place for pc-anti-RO as well, but to a lesser extent than with psiPNA (Figure 6b, lower gel). These observations agree with the hypothesis that only psiPNA is able to invade dsDNA under isothermal conditions. Full dehybridization of the PGR-RO, however, can only be

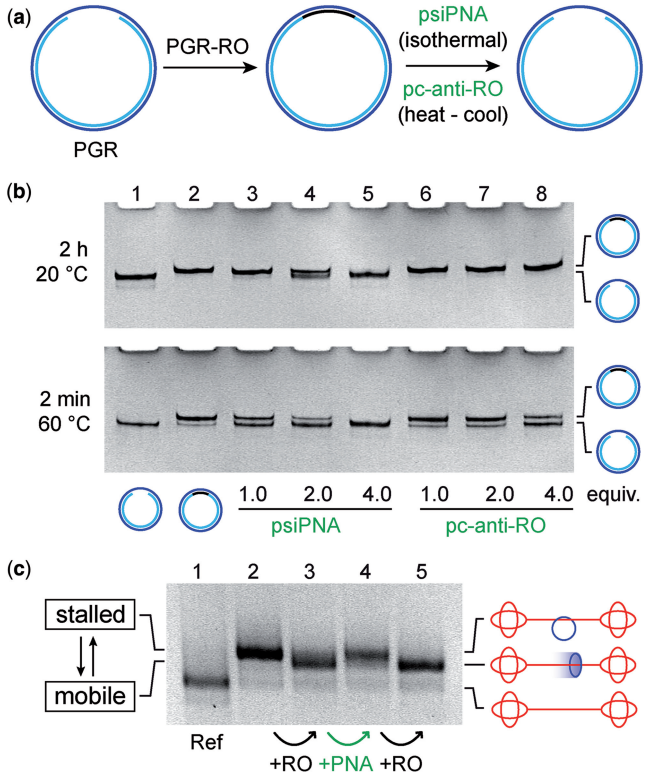

Figure 6. Experimental setup of the macrocycle invasion study. (**a**) In the first step, PGR-RO (black) hybridizes to the gap ring (blue) to form a completely double-stranded DNA nanoring. In the second step, psiPNA (green) invades the dsDNA nanoring and detaches PGR-RO from the gap ring while psiPNA•PGR-RO is formed as waste. To demonstrate the influence of PNA in the isothermal displacement reaction, an analogous experiment is performed with the corresponding DNA pc-anti-RO (green). (**b**) Polyacrylamide gels (10%) of the macrocycle invasion studies. Upper gel: after incubation of the macrocycle for 2 h at 20°C. Lane 1: PGR (reference). Lane 2: PGR•PGR-RO nanoring. Lane 3–5: dsDNA nanoring incubated with 1.0, 2.0 and 4.0 equivalents of psiPNA. Lane 6–8: dsDNA nanoring incubated with 1.0, 2.0 and 4.0 equivalents of pc-anti-RO. According to the band intensities in lane 5, the 14-mer PGR-RO (black) is nearly quantitatively removed from the gap ring, whereas the presence of pc-anti-RO had no influence on the macrocycle. Lower gel: after incubation of the macrocycle for 24 h at 20°C and then 2 min at 60°C. After annealing, these conditions lead to the thermodynamically equilibrium state between all components, as reflected by the ratio of the band intensities between full macrocycle and free gap-ring. (**c**) PGR-RO/psiPNA triggered reversible pseudorotaxane/rotaxane reconfiguration followed by agarose gel (2.4%). Lane 1: DNA dumbbell (reference). Lane 2: pseudorotaxane (HPLC purified, see main text). Lane 3: addition of PGR-RO (2.0 equivalents; black arrow) detaches the macrocycle from the dumbbell to form the rotaxane. Lane 4: addition of psiPNA (8.0 equivalents; green arrow) reverts the process and the pseudorotaxane is reconstructed. Lane 5: treating the sample with another 10.0 equivalents of PGR-RO (black arrow), the rotaxane band reappears on gel. The band intensities in lanes 2–5 indicate nearly quantitative conversion at each switching event.

achieved after heating the samples to 60°C, followed by annealing under thermodynamic control to the given band intensities of full macrocycle vs. free gap ring (Figure 6b, lower gel; Supplementary Figure S5 for full series of gels). Surprisingly, the displacement of PGR-RO does not work quantitatively using a 1:1 stoichiometry. We assume that psiPNA tends to form aggregates in a rather slow process, and therefore, not all added psiPNA is accessible in the actual strand displacement process. This hypothesis is supported by the fact that psiPNA must be completely denatured by warming up to 95°C for 1 min right before it is added to the sample. Otherwise, more equivalents of psiPNA are required for efficient strand displacement, or after longer periods like 3 days, high-molecular-weight aggregates of DNA gap rings are observed (data not shown).

Building up on the displacement result mentioned previously, we applied the pcPNA-directed switching system to the rotaxane architecture. The switching operations were again observed by gel-shift analysis that discriminates between the immobile pseudorotaxane state and the mobile rotaxane state, as we have unequivocally demonstrated previously (26,27,41) (Figure 6c; lane 1 shows the related dumbbell as a reference). In the initial step, the immobile macrocycle (pseudorotaxane, lane 2) was released from the dumbbell by 2.0 equivalents of PGR-RO. Within <30 min, the genuine rotaxane with fully mobile components is formed (lane 3). To fix the macrocycle back to the axle, 8.0 equivalents of psiPNA were added and incubated overnight at ambient temperature (lane 4). By addition of 10.0 equivalents of PGR-RO, the bound macrocycle could be switched back again into the rotaxane state (lane 5), further underscoring the reversibility of the switching. The respective band intensities in the different lanes indicate that the individual switching operations occur nearly quantitatively. Moreover, the last switching event indicates that, in principle, it is possible to perform many more of these operations.

CONCLUSIONS

The switching system introduced here illustrates that reversible structural rearrangements of complex DNA architectures are possible on the basis of pcPNA. Although the switching performance appears to be somewhat less robust than the light-induced switching (27), the pcPNA-based switching strategy complements the toolbox of switches in DNA nanotechnology that can be combined with other methods of strand replacement such as light or toehold switches in an orthogonal fashion. Importantly, the operation of the pcPNA switch that occurs through a relatively slow double-strand invasion mechanism works under isothermal conditions. Analogous pcDNA sequences do not show any displacement behaviour at 20°C. However, on the one hand, the use of pc nucleobases could be of interest in toehold-based switching systems, and on the other, the toehold principle might be applicable to PNA sequences as well. Until now, PNA has experienced only limited application in DNA nanotechnology. For example, bis-PNA sequences were used to connect two DNA single strands through Watson–Crick pairing patterns (65). PNA was also used to associate gold nanoparticles with a dsDNA through strand invasion (66), which in this case, however, was associated with certain restrictions in the sequence and did not occur isothermally. Another example reported the assembly of two-dimensional arrays by means of hybrid PNA/DNA tiles (67). In all of these examples, the PNA was integrated into the target structure. The

here-described method that uses pcPNA to operate a nanomechanical switch in a DNA architecture through strand exchange is unprecedented. We do not use the PNA as an integral component of the nanoarchitecture, but as an actuator that triggers structural rearrangements in a DNA architecture. The invasive character of the pcPNA drives the switch into the desired direction. The switching itself can be programmed without ambiguity by introducing pc nucleobases into the architecture, and thus rests on a clear design strategy. Based on a toehold-free switching principle, pcPNAs can potentially be combined with light- and toehold-based switches, thus opening up new avenues in dynamic DNA nanotechnology.

SUPPLEMENTARY DATA

Supplementary Data are available at NAR Online: Supplementary Table 1, Supplementary Figures 1–5 and Supplementary Methods.

ACKNOWLEDGEMENTS

The authors thank Klaus Rotscheidt for help with the PNA solid-phase synthesis.

FUNDING

European Research Council [ERC Advanced Grant 267173] and the Deutsche Forschungsgemeinschaft DFG. Funding for open access charge: ERC Advanced [267173].

Conflict of interest statement. None declared.

REFERENCES

1. Wickham,S.F., Bath,J., Katsuda,Y., Endo,M., Hidaka,K., Sugiyama,H. and Turberfield,A.J. (2012) A DNA-based molecular motor that can navigate a network of tracks. *Nat. Nanotechnol.*, **7**, 169–173.
2. Douglas,S.M., Bachelet,I. and Church,G.M. (2012) A logic-gated nanorobot for targeted transport of molecular payloads. *Science*, **335**, 831–834.
3. Zhang,Z., Olsen,E.M., Kryger,M., Voigt,N.V., Tørring,T., Gültekin,E., Nielsen,M., Mohammadzadegan,R., Andersen,E.S., Nielsen,M.M. *et al.* (2011) A DNA tile actuator with eleven discrete states. *Angew. Chem. Int. Ed. Engl.*, **50**, 3983–3987.
4. Wickham,S.F., Endo,M., Katsuda,Y., Hidaka,K., Bath,J., Sugiyama,H. and Turberfield,A.J. (2011) Direct observation of stepwise movement of a synthetic molecular transporter. *Nat. Nanotechnol.*, **6**, 166–169.
5. Muscat,R.A., Bath,J. and Turberfield,A.J. (2011) A programmable molecular robot. *Nano Lett.*, **11**, 982–987.
6. He,Y. and Liu,D.R. (2010) Autonomous multistep organic synthesis in a single isothermal solution mediated by a DNA walker. *Nat. Nanotechnol.*, **5**, 778–782.
7. Han,D., Pal,S., Liu,Y. and Yan,H. (2010) Folding and cutting DNA into reconfigurable topological nanostructures. *Nat. Nanotechnol.*, **5**, 712–717.
8. Omabegho,T., Sha,R. and Seeman,N.C. (2009) A bipedal DNA brownian motor with coordinated legs. *Science*, **324**, 67–71.
9. Zhang,D.Y. and Seelig,G. (2011) Dynamic DNA nanotechnology using strand-displacement reactions. *Nat. Chem.*, **3**, 103–113.
10. Pinheiro,A.V., Han,D., Shih,W.M. and Yan,H. (2011) Challenges and opportunities for structural DNA nanotechnology. *Nat. Nanotechnol.*, **6**, 763–772.
11. Krishnan,Y. and Simmel,F.C. (2011) Nucleic acid based molecular devices. *Angew. Chem. Int. Ed. Engl.*, **50**, 3124–3156.
12. Bath,J. and Turberfield,A.J. (2007) DNA nanomachines. *Nat. Nanotechnol.*, **2**, 275–284.
13. Elbaz,J., Wang,Z.G., Wang,F. and Willner,I. (2012) Programmed dynamic topologies in DNA catenanes. *Angew. Chem. Int. Ed. Engl.*, **51**, 2349–2353.
14. Goodman,R.P., Heilemann,M., Doose,S., Erben,C.M., Kapanidis,A.N. and Turberfield,A.J. (2008) Reconfigurable, braced, three-dimensional DNA nanostructures. *Nat. Nanotechnol.*, **3**, 93–96.
15. Yan,H., Zhang,X., Shen,Z. and Seeman,N. (2002) A robust DNA mechanical device controlled by hybridization topology. *Nature*, **415**, 62–65.
16. Yurke,B., Turberfield,A., Mills,A., Simmel,F. and Neumann,J. (2000) A DNA-fuelled molecular machine made of DNA. *Nature*, **406**, 605–608.
17. Zhang,D.Y. and Winfree,E. (2009) Control of DNA strand displacement kinetics using toehold exchange. *J. Am. Chem. Soc.*, **131**, 17303–17314.
18. Andersen,E.S., Dong,M., Nielsen,M.M., Jahn,K., Subramani,R., Mamdouh,W., Golas,M.M., Sander,B., Stark,H., Oliveira,C.L. *et al.* (2009) Self-assembly of a nanoscale DNA box with a controllable lid. *Nature*, **459**, 73–76.
19. Genot,A.J., Zhang,D.Y., Bath,J. and Turberfield,A.J. (2011) Remote toehold: a mechanism for flexible control of DNA hybridization kinetics. *J. Am. Chem. Soc.*, **133**, 2177–2182.
20. Chen,X. (2012) Expanding the rule set of DNA circuitry with associative toehold activation. *J. Am. Chem. Soc.*, **134**, 263–271.
21. Liang,X., Nishioka,H., Takenaka,N. and Asanuma,H. (2008) A DNA nanomachine powered by light irradiation. *Chembiochem*, **9**, 702–705.
22. Hara,Y., Fujii,T., Kashida,H., Sekiguchi,K., Liang,X., Niwa,K., Takase,T., Yoshida,Y. and Asanuma,H. (2010) Coherent quenching of a fluorophore for the design of a highly sensitive in-stem molecular beacon. *Angew. Chem. Int. Ed. Engl.*, **49**, 5502–5506.
23. Zhou,M., Liang,X., Mochizuki,T. and Asanuma,H. (2010) A light-driven DNA nanomachine for the efficient photoswitching of RNA digestion. *Angew. Chem. Int. Ed. Engl.*, **49**, 2167–2170.
24. Hayashi,H., Liang,X., Zhao,J., Komiyama,M. and Asanuma,H. (2006) Activation of DNA enzyme 10-23 by tethering an intercalator to its backbone. *Nucleic Acids Symp. Ser. (Oxf).*, 167–168.
25. Han,D., Huang,J., Zhu,Z., Yuan,Q., You,M., Chen,Y. and Tan,W. (2011) Molecular engineering of photoresponsive three-dimensional DNA nanostructures. *Chem. Commun.*, **47**, 4670–4672.
26. Ackermann,D., Schmidt,T.L., Hannam,J.S., Purohit,C.S., Heckel,A. and Famulok,M. (2010) A double-stranded DNA rotaxane. *Nat. Nanotechnol.*, **5**, 436–442.
27. Lohmann,F., Ackermann,D. and Famulok,M. (2012) A reversible light switch for macrocycle mobility in a DNA rotaxane. *J. Am. Chem. Soc.*, **134**, 11884–11887.
28. Nishioka,H., Liang,X., Kato,T. and Asanuma,H. (2012) A photon-fueled DNA nanodevice that contains two different photoswitches. *Angew. Chem. Int. Ed. Engl.*, **51**, 1165–1168.
29. Zhang,C., Tian,C., Li,X., Qian,H., Hao,C., Jiang,W. and Mao,C. (2012) Reversibly switching the surface porosity of a DNA tetrahedron. *J. Am. Chem. Soc.*, **134**, 11998–12001.
30. Kutyavin,I.V., Rhinehart,R.L., Lukhtanov,E.A., Gorn,V.V., Meyer,R.B. and Gamper,H.B. (1996) Oligonucleotides containing 2-aminoadenine and 2-thiothymine act as selectively binding complementary agents. *Biochemistry*, **35**, 11170–11176.
31. Hoshika,S., Chen,F., Leal,N.A. and Benner,S.A. (2010) Artificial genetic systems: self-avoiding DNA in PCR and multiplexed PCR. *Angew. Chem. Int. Ed. Engl.*, **49**, 5554–5557.
32. Lohse,J., Dahl,O. and Nielsen,P. (1999) Double duplex invasion by peptide nucleic acid: a general principle for sequence-specific targeting of double-stranded DNA. *Proc. Natl Acad. Sci. USA*, **96**, 11804–11808.
33. Haaima,G., Hansen,H., Christensen,L., Dahl,O. and Nielsen,P. (1997) Increased DNA binding and sequence discrimination of

PNA oligomers containing 2,6-diaminopurine. *Nucleic Acids Res.*, **25**, 4639–4643.
34. Porcheddu,A. and Giacomelli,G. (2005) Peptide nucleic acids (PNAs), a chemical overview. *Curr. Med. Chem.*, **12**, 2561–2599.
35. Demidov,V. and Frank-Kamenetskii,M. (2004) Two sides of the coin: affinity and specificity of nucleic acid interactions. *Trends Biochem. Sci.*, **29**, 62–71.
36. Nielsen,P. and Haaima,G. (1997) Peptide nucleic acid (PNA). A DNA mimic with a pseudopeptide backbone. *Chem. Soc. Rev.*, **26**, 73–78.
37. Christensen,L., Fitzpatrick,R., Gildea,B., Petersen,K.H., Hansen,H.F., Koch,T., Egholm,M., Buchardt,O., Nielsen,P.E. and Coull,J. (1995) Solid-phase synthesis of peptide nucleic acids. *J. Pept. Sci.*, **1**, 175–183.
38. Smolina,I. and Demidov,V. (2003) Sequence-universal recognition of duplex DNA by oligonucleotides via pseudocomplementarity and helix invasion. *Chem. Biol.*, **10**, 591–595.
39. Demidov,V., Protozanova,E., Izvolsky,K., Price,C., Nielsen,P. and Frank-Kamenetskii,M. (2002) Kinetics and mechanism of the DNA double helix invasion by pseudocomplementary peptide nucleic acids. *Proc. Natl Acad. Sci. USA*, **99**, 5953–5958.
40. Abibi,A., Protozanova,E., Demidov,V.V. and Frank-Kamenetskii,M.D. (2008) Specific versus nonspecific binding of cationic PNAs to duplex DNA. *Biophys. J.*, **86**, 3070–3078.
41. Ackermann,D., Jester,S.S. and Famulok,M. (2012) Design strategy for DNA rotaxanes with a mechanically reinforced PX100 axle. *Angew. Chem. Int. Ed. Engl.*, **51**, 6771–6775.
42. Yerin,A., Wilks,E.S., Moss,G.P. and Harada,A. (2008) Nomenclature for rotaxanes and pseudorotaxanes - (IUPAC recommendations 2008). *Pure Appl. Chem.*, **80**, 2041–2068.
43. Wittung,P., Nielsen,P. and Norden,B. (1996) Direct observation of strand invasion by peptide nucleic acid (PNA) into double-stranded DNA. *J. Am. Chem. Soc.*, **118**, 7049–7054.
44. Demidov,V., Yavinlovich,M., Belotserkovskii,B., Frank-Kamenetskii,M. and Nielsen,P. (1995) Kinetics and mechanism of polyamide (peptide) nucleic-acid binding to duplex DNA. *Proc. Natl Acad. Sci. USA*, **92**, 2637–2641.
45. Peffer,N., Hanvey,J., Bisi,J., Thomson,S., Hassman,C., Noble,S. and Babiss,L. (1993) Strand-invasion of duplex DNA by peptide nucleic-acid oligomers. *Proc. Natl Acad. Sci. USA*, **90**, 10648–10652.
46. Komiyama,M., Aiba,Y., Ishizuka,T. and Sumaoka,J. (2008) Solid-phase synthesis of pseudo-complementary peptide nucleic acids. *Nat. Protoc.*, **3**, 646–654.
47. Ackermann,D. and Pitsch,S. (2002) Synthesis and pairing properties of 3′-deoxyribopyranose (4′, 2′)-oligonucleotides ('p-DNA'). *Helv. Chim. Acta*, **85**, 1443–1462.
48. Yamamoto,Y., Yoshida,J., Tedeschi,T., Corradini,R., Sforza,S. and Komiyama,M. (2006) Highly efficient strand invasion by peptide nucleic acid bearing optically pure lysine residues in its backbone. *Nucleic Acids Symp. Ser. (Oxf).*, 109–110.
49. Kaihatsu,K., Shah,R., Zhao,X. and Corey,D. (2003) Extending recognition by peptide nucleic acids (PNAs): binding to duplex DNA and inhibition of transcription by tail-clamp PNA-Peptide conjugates. *Biochemistry*, **42**, 13996–14003.
50. Kuhn,H., Demidov,V., Frank-Kamenetskii,M. and Nielsen,P. (1998) Kinetic sequence discrimination of cationic bis-PNAs upon targeting of double-stranded DNA. *Nucleic Acids Res.*, **26**, 582–587.
51. Griffith,M., Risen,L., Greig,M., Lesnik,E., Sprankle,K., Griffey,R., Kiely,J. and Freier,S. (1995) Single and bis peptide nucleic-acids as triplexing agents - binding and stoichiometry. *J. Am. Chem. Soc.*, **117**, 831–832.
52. Wittung,P., Nielsen,P., Buchardt,O., Egholm,M. and Norden,B. (1994) DNA-like double helix formed by peptide nucleic-acid. *Nature*, **368**, 561–563.
53. Schnolzer,M., Alewood,P., Jones,A., Alewood,D. and Kent,S.B. (1992) In situ neutralization in Boc-chemistry solid phase peptide synthesis. Rapid, high yield assembly of difficult sequences. *Int. J. Pept. Protein Res.*, **40**, 180–193.
54. Shigeta,S., Mori,S., Watanabe,F., Takahashi,K., Nagata,T., Koike,N., Wakayama,T. and Saneyoshi,M. (2002) Synthesis and antiherpesvirus activities of 5-alkyl-2-thiopyrimidine nucleoside analogues. *Antivir. Chem. Chemother.*, **13**, 67–82.
55. Connolly,B. and Newman,P. (1989) Synthesis and properties of oligonucleotides containing 4-thiothymidine, 5-methyl-2-pyrimidinone-1-beta-D(2'-deoxyriboside) and 2-thiothymidine. *Nucleic Acids Res.*, **17**, 4957–4974.
56. Kuimelis,R., Hope,H. and Nambiar,K. (1993) A stereoselective synthesis of alpha-2'-deoxy-2-thiouridine and beta 2'-deoxy-2-thiouridine. *Nucleosides Nucleotides Nucleic Acids*, **12**, 737–755.
57. Vorbrüggen,H. and Strehlke,P. (1973) Synthesis of nucleosides.7. New synthesis of 2-thiopyrimidine nucleosides. *Chem. Ber.*, **106**, 3039–3061.
58. Gemmel,C., Janairo,G., Kilburn,J., Ueck,H. and Underhill,A. (1994) Synthesis of unsymmetrical tetrakis(alkylsulfanyl)tetrathiafulvalene derivatives. *J. Chem. Soc. Perk. T.*, **1**, 2715–2720.
59. Taylor,L., Grasshoff,J. and Pluhar,M. (1978) Use of ortho-hydroxybenzyl and para-hydroxybenzyl functions as blocking groups wich are removable with base. *J. Org. Chem.*, **43**, 1197–1200.
60. Wierenga,W. and Skulnick,H. (1981) Investigations of the mechanism of nucleosides synthesis .2. Stereochemical control as a function of protecting-group participation in 2-deoxy-D-erythro-pentofuranosyl nucleosides. *Carbohydr. Res.*, **90**, 41–52.
61. Kumar,R. and Davis,D. (1995) Synthesis of oligoribonucleotides containing 2-thiouridine - Incorporation of 2-thiouridine phosphoramidite without base protection. *J. Org. Chem.*, **60**, 7726–7727.
62. Kuimelis,R. and Nambiar,K. (1994) Synthesis of oligodeoxynucleotides containing 2-thiopyrimidine residues - a new protection scheme. *Nucleic Acids Res.*, **22**, 1429–1436.
63. Sochacka,E. (2001) Efficient assessment of modified nucleoside stability under conditions of automated oligonucleotide synthesis: characterization of the oxidation and oxidative desulfurization of 2-thiouridine. *Nucleosides Nucleotides Nucleic Acids*, **20**, 1871–1879.
64. Rasched,G., Ackermann,D., Schmidt,T.L., Broekmann,P., Heckel,A. and Famulok,M. (2008) DNA minicircles with gaps for versatile functionalization. *Angew. Chem. Int. Ed. Engl.*, **47**, 967–970.
65. Nulf,C. and Corey,D. (2002) DNA assembly using bis-peptide nucleic acids (bisPNAs). *Nucleic Acids Res.*, **30**, 2782–2789.
66. Stadler,A.L., Sun,D., Maye,M.M., van der Lelie,D. and Gang,O. (2011) Site-selective binding of nanoparticles to double-stranded DNA via peptide nucleic acid "invasion". *ACS Nano*, **5**, 2467–2474.
67. Lukeman,P., Mittal,A. and Seeman,N. (2004) Two dimensional PNA/DNA arrays: estimating the helicity of unusual nucleic acid polymers. *Chem. Commun. (Camb)*, 1694–1695.